Supplemental Information

Structural Analysis Reveals Features of Ribosome Assembly Factor Nsa1/WDR74 Important for Localization and Interaction with Rix7/NVL2

Yu-Hua Lo, Erin M. Romes, Monica C. Pillon, Mack Sobhany, and Robin E. Stanley

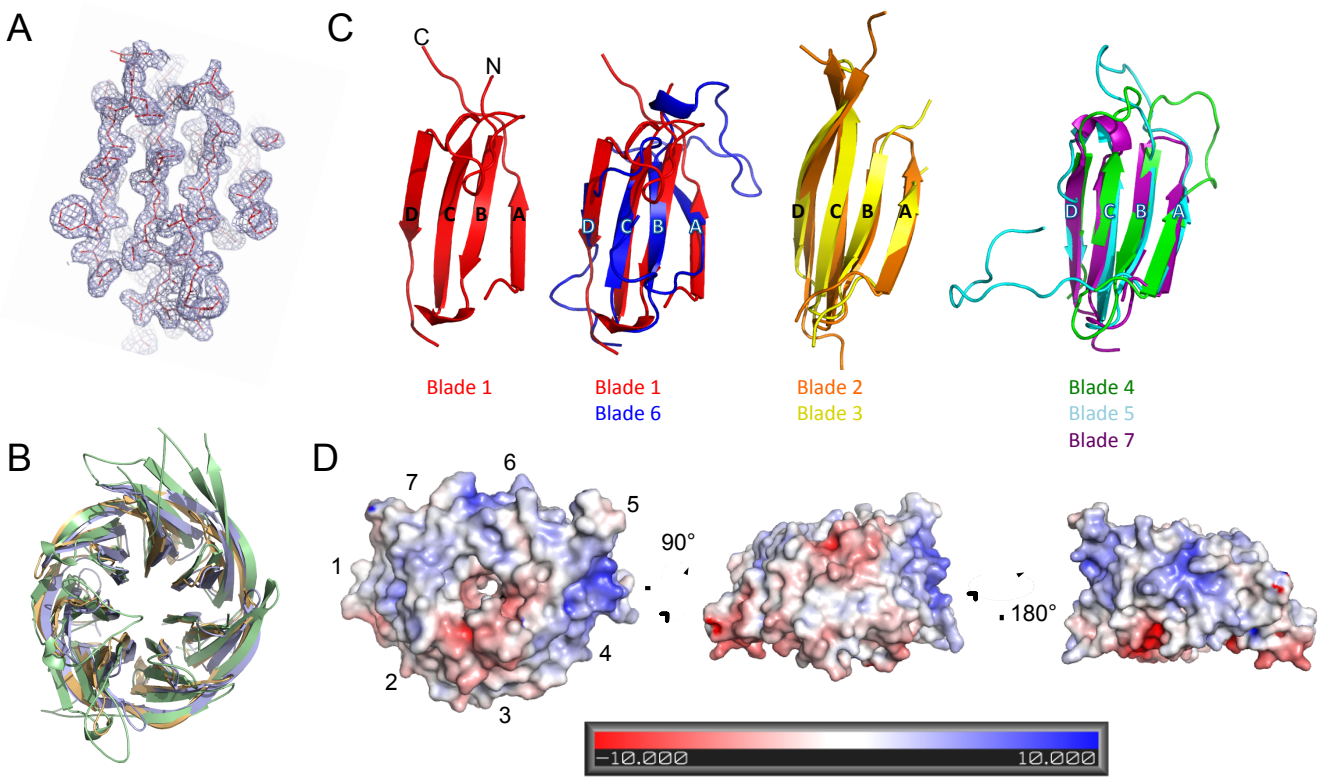

Figure S1. Comparison of the individual Nsa1 blades (related to Figure 1) (A) Experimental electron density map derived from SAD phasing and contoured at 1.2 sigma. This map covers blade number 1 at a resolution of 1.7 Å. (B) Superposition of Nsa1 (green) with PDBID 1RI6 (orange) and PDBID 1JOF(blue), the top two hits from the DALI search. (C) Comparison of the individual blades of Nsa1$_{\Delta C}$ (PDB 5SUI). (D) Vacuum electrostatic surface potential representation of the WD40 domain of Nsa1 calculated using the APBS module within PyMol. Positively charged surfaces are shown in blue and negatively charged surfaces are shown in red.

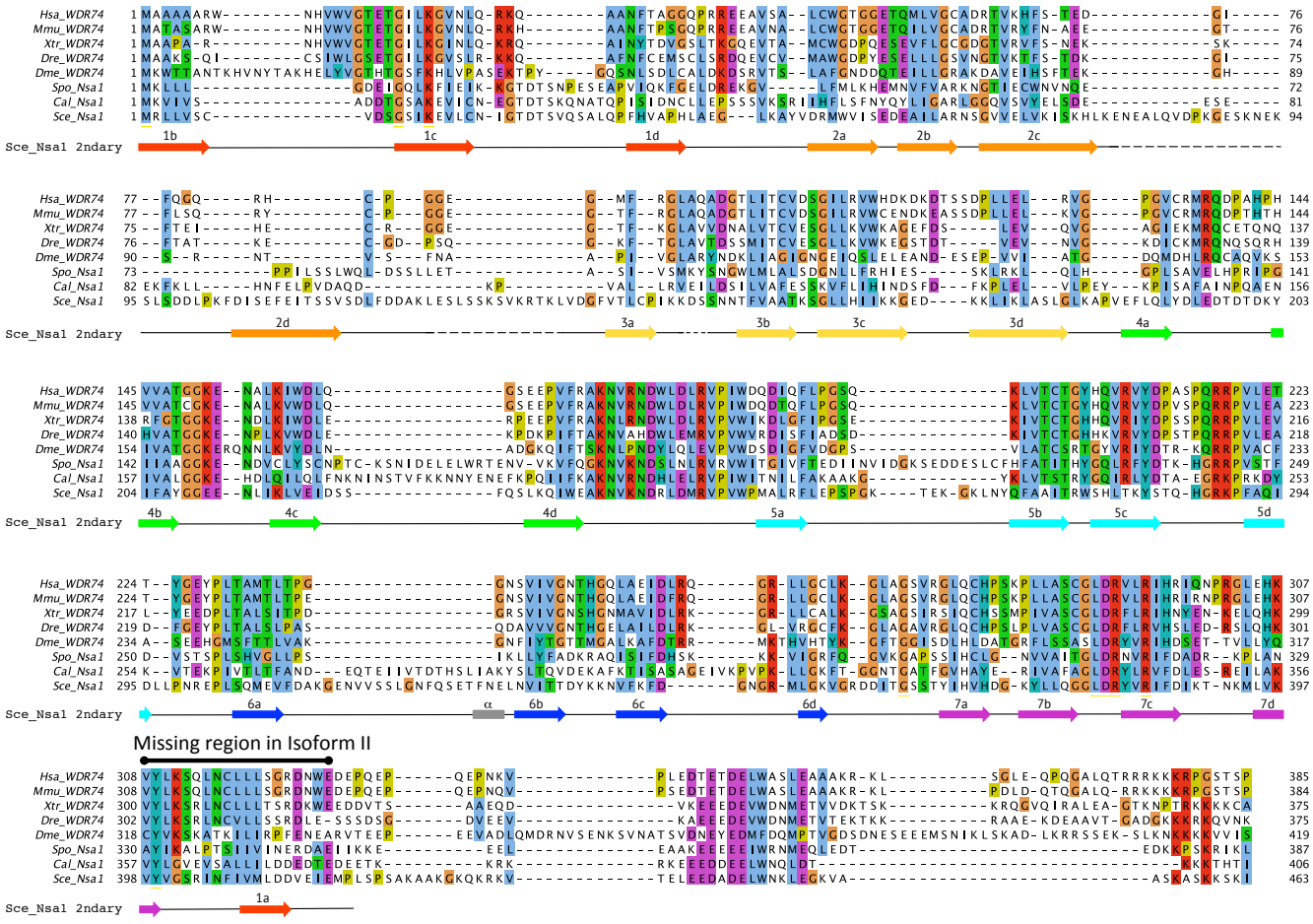

Figure S2. Multiple sequence alignment of Nsa1/WDR74 from different homologues of *Homo sapiens* (*Hsa*), *Mus musculus* (*Mmu*), *Xenopus tropicalis* (*Xtr*), *Danio rerio* (*Dre*) *Drosophila melanogaster* (*Dme*), *Schizosaccharomyces pombe* (*Spo*), *Candida albicans* (*Cal*), and *Saccharomyces cerevisiae* (*Sce*) (related to Figure 1). The alignment was done in Tcoffee and colored with Jalview. *Sce* Nsa1 contains several long loops not found in other species so the alignment was adjusted manually within blade 6. The secondary structure of *Sce* Nsa1 determined by the crystal structure is shown below the sequence. Black bold line indicates the miss region in C-terminus of *Has* WDR74 isoform II.

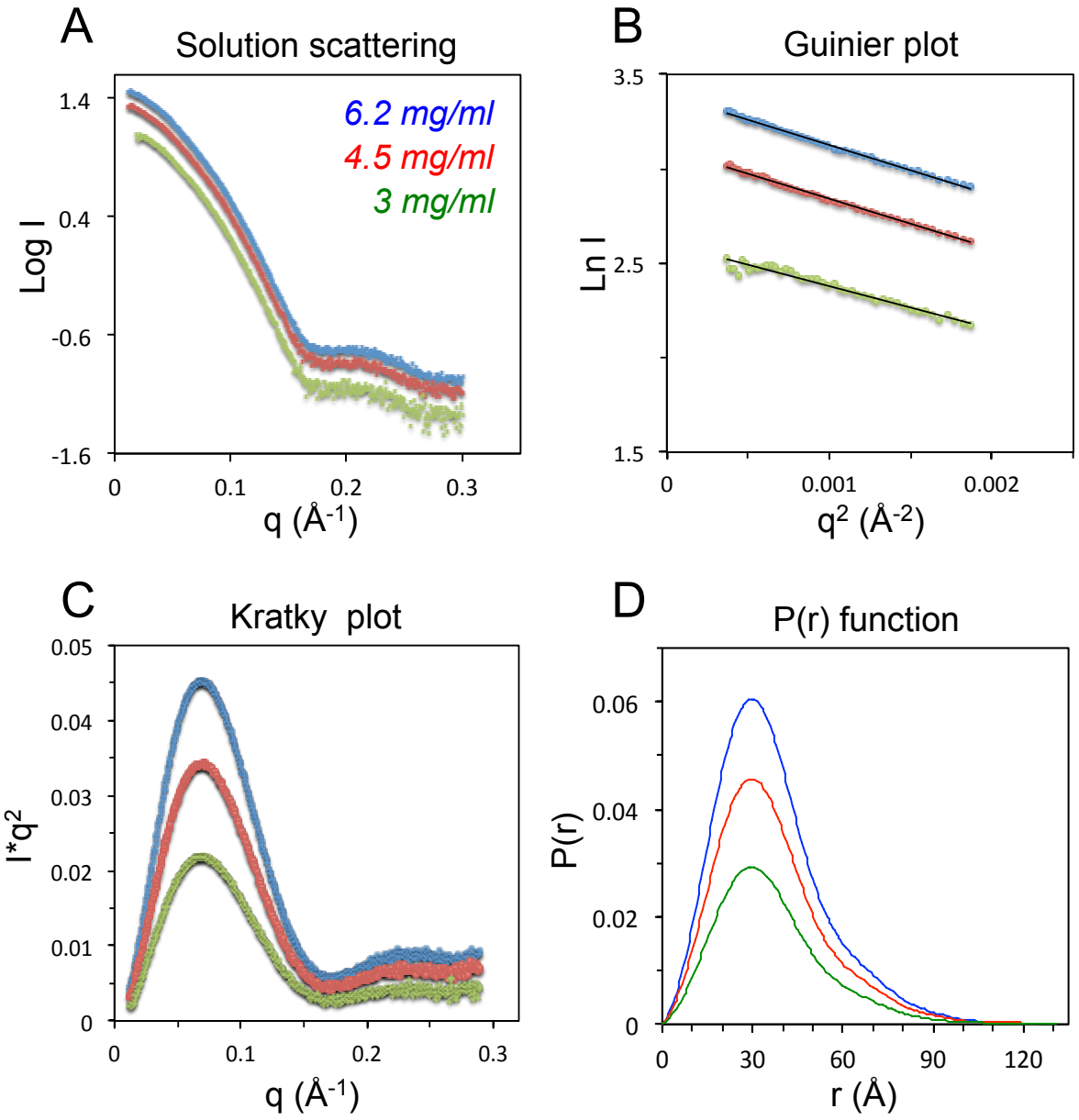

Figure S3. SAXS analysis of *Sce* Nsa1$_{FL}$ at three different protein concentrations (related to Figure 2) (A) Experimental scattering curve of Nsa1 at 6.2 (blue, open circles), 4.5 (red, open circles), and 3 (green, open circles) mg/ml (B) Guinier region and linear regression (black solid line) are used to determine the radius of gyration (Rg) shown in Table S1. The linearity of the Guinier plots indicates the absence of interparticle interactions. (C) Kratky plots of Nsa1 show the protein is folded in solution. (D) Pair-distance distribution functions were generated using Gnom. The Nsa1 concentration series (6.2-3 mg/ml) had a calculated D_{max} value of 125 Å, 125 Å, and 132 Å, respectively (see Table S1).

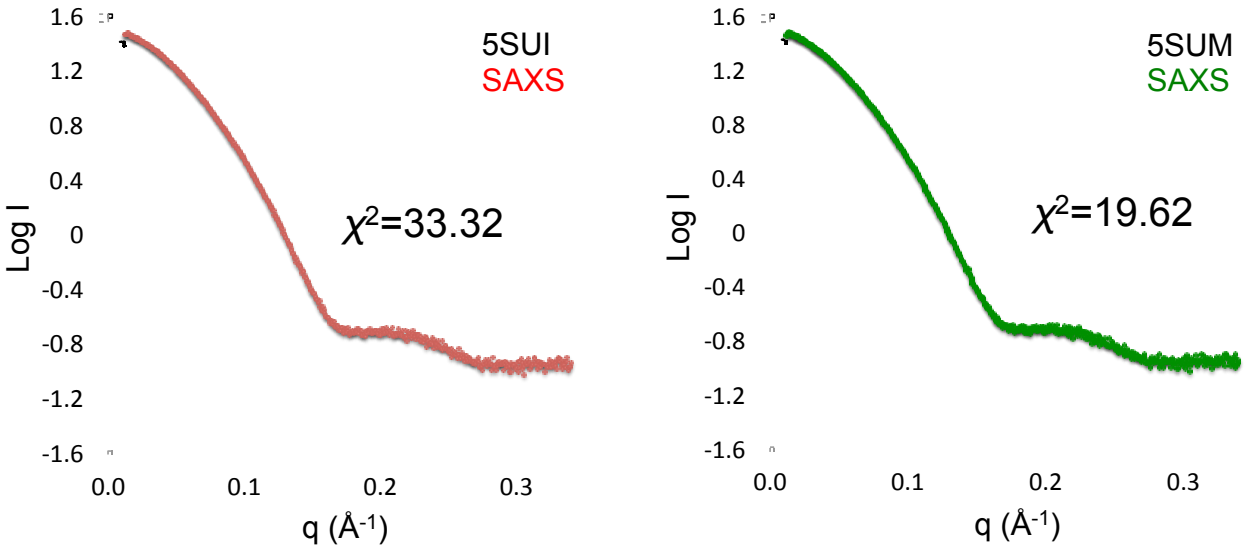

Figure S4. Comparing Nsa1 crystal structures to solution scattering data (related to Figure 2). Discrepancy of the theoretical scattering curve of $Nsa1_{FL}$ with our crystal structures.

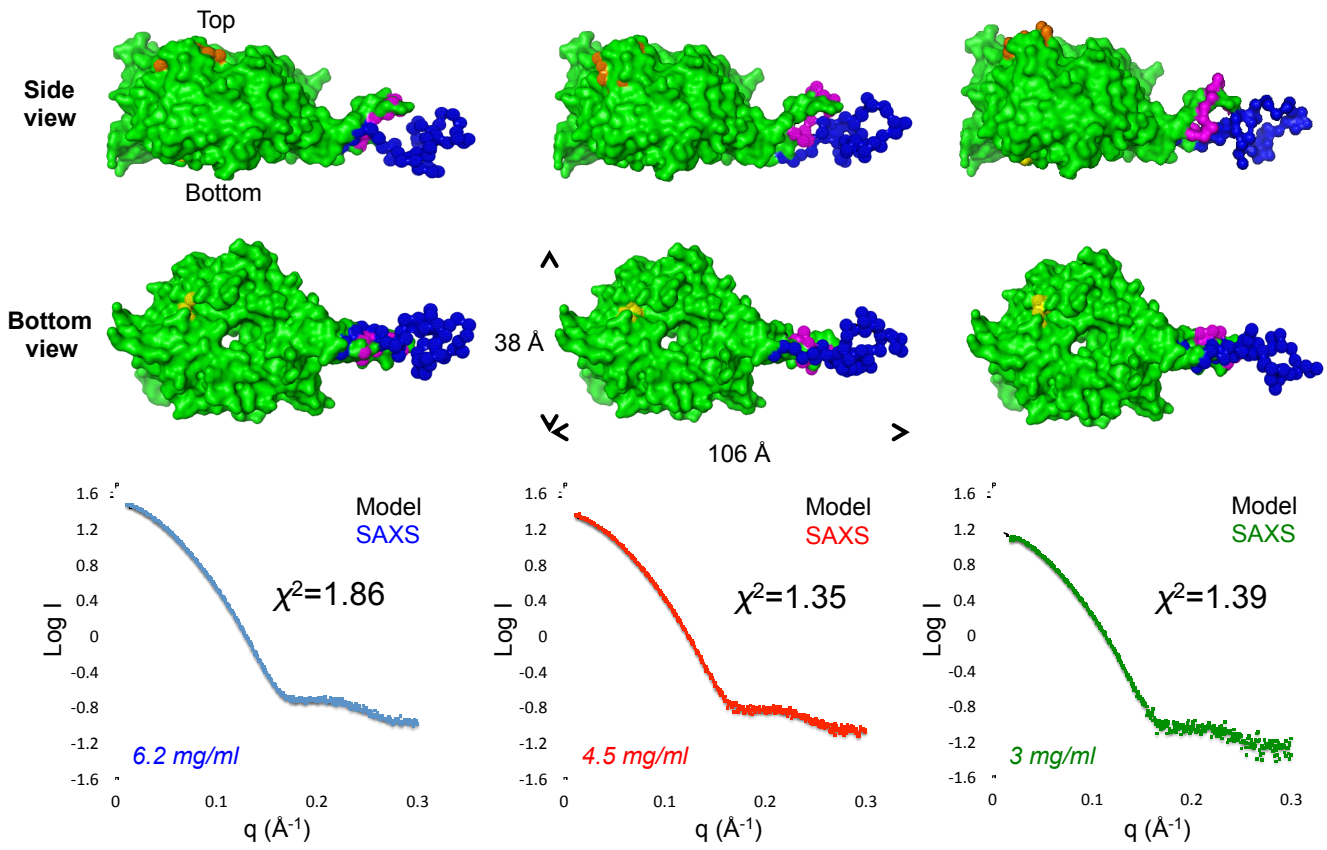

Figure S5. Bunch models of *Sce* Nsa1$_{FL}$ (related to Figure 2) (Top) The rigid body model of *Sce* Nsa1$_{FL}$ determined by Bunch using the scattering curve from each Nsa1$_{FL}$ concentration. The C-terminus (418-463) is colored in blue, whereas the modeled loops (85-98, 125-136, 196-202) missing from the crystal structures are colored in purple, orange and yellow, respectively. (Bottom) Discrepancy of the theoretical scattering curve from the Nsa1$_{FL}$ model generated in Bunch to the experimental solution scattering profile at three concentrations (6.2-3 mg/ml) have chi^2 of 1.86, 1.35 and 1.39, respectively.

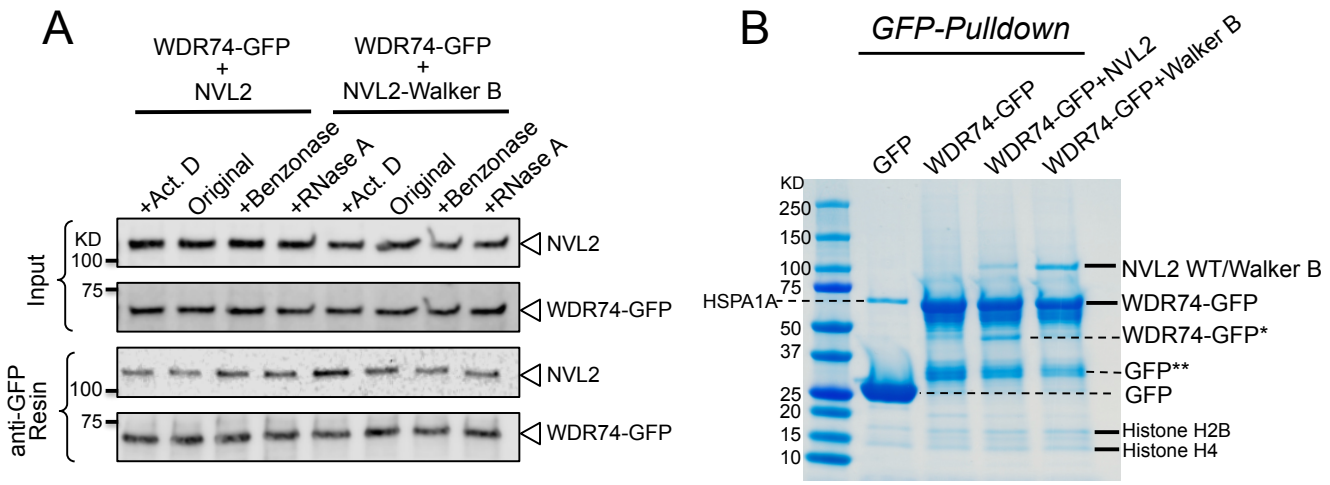

Figure S6

Figure S6. The WDR74-NVL2 interaction is RNA independent (related to Figure 3) (A) Western blot analysis of the interaction between WDR74 and NVL2 with different conditions of cell treatment. Act. D: Cells were treated with low concentrations of actinomycin D for 2 hours prior to harvesting which causes an arrest of rRNA synthesis thereby inhibiting ribosome biogenesis. Original: Standard co-immunoprecipitation conditions as described in the methods, +Benzonase: Addition of Benzonase in both cell lysis buffer and wash buffer. +RNase A: Addition of both RNase A and Benzonase in both cell lysis buffer and wash buffer. Co-immunoprecipitation experiments were carried out with the wild-type and Walker-B mutant NVL2 (E364Q/E681Q) which impairs ATP hydrolysis. (B) Large-scale WDR74-GFP co-immunoprecipitations analyzed by SDS-PAGE with coomassie-staining. The proteins identified by mass spectrometry are indicated. The WDR74-GFP* represents a degradation product of WDR74-GFP, whereas GFP** represents free GFP with a linker sequence from our plasmid.

Table S1, related to STAR Methods. SAXS data-collection and scattering-derived parameters for full-length *Sce* Nsa1

	S. cerevisiae $Nsa1_{FL}$		
Data-collection parameters			
Concentration (mg/ml)	6.2	4.5	3.0
Exposure time (sec)	0.3	0.3	0.3
Structural parameters			
I_0 (cm^{-1}) [from Guinier]	29.29 ± 0.07	22.00 ± 0.05	13.95 ± 0.04
R_g (Å) [from Guinier]	27.65 ± 0.09	27.51 ± 0.09	27.29 ± 0.12
I_0 (cm^{-1}) [fromP(r)]	29.43	22.23	14.14
R_g (Å) [from P(r)]	28.54	28.70	28.53
Dmax (Å)	125	125	132
Experimental MW [from Q_R][a]	51,781	51,729	52,277
Theoretical MW[b]	52,310	52,310	52,310
χ^2 of Bunch models	1.86	1.35	1.39

[a]MW determined using ScÅtter (Rambo and Tainer, 2013)
[b]Theoretical MW of Nsa1 (MBP tag cleaved by TEV)

Supplemental References

Rambo, R.P., and Tainer, J.A. (2013). Accurate assessment of mass, models and resolution by small-angle scattering. Nature *496*, 477-481.